

Non-axisymmetric dynamic response of buried orthotropic cylindrical shells under moving load

V.P. Singh†, J.P. Dwivedi† and P.C. Upadhyay‡

*Department of Mechanical Engineering, Institute of Technology,
Banaras Hindu University, VARANASI-221005, India*

Abstract. The dynamic response of buried pipelines has gained considerable importance because these pipelines perform vital role in conducting energy, water, communication and transportation. After realizing the magnitude of damage, and hence, the human uncomfot and the economical losses, researchers have paid sincere attention to this problem. A number of papers have appeared in the past which discuss the different aspects of the problem. This paper presents a theoretical analysis of non-axisymmetric dynamic response of buried orthotropic cylindrical shell subjected to a moving load along the axis of the shell. The orthotropic shell has been buried in a homogeneous, isotropic and elastic medium of infinite extent. A thick shell theory including the effects of rotary inertia and shear deformation has been used. A perfect bond between the shell and the surrounding medium has been assumed. Results have been obtained for very hard (rocky), medium hard and soft soil surrounding the shell. The effects of shell orthotropy have been brought out by varying the non-dimensional orthotropic parameters over a long range. Under these conditions the shell response is studied in axisymmetric mode as well as in the flexural mode. It is observed that the shell response is significantly affected by change in orthotropic parameters and also due to change of response mode. It is observed that axial deformation is large in axisymmetric mode as compared to that in flexural mode.

Key words: buried pipelines; cylindrical shell; dynamic response; moving load; non-axisymmetric response.

1. Introduction

During the last 15 years, a good deal of research interest has been generated in the dynamic response of buried pipelines subjected to radial moving load. As they perform a vital role in modern day life, any damage to these buried pipelines may cause sufferings to mankind over a vast area. The moving load in the axial direction along the interior of the pipeline is one of the prominent source of excitation to buried pipelines. It has been shown in the past that the treatment of pipeline as buried cylindrical shell gives the better ways of explaining the nature of pipe failures (Singh *et al.* 1987).

The problem of dynamic response of a cylindrical shell subjected to a moving load has gained considerable importance in the fields of mechanical, civil and in particular aerospace engineering. Structures such as rocket, aeroplanes and submarines are subjected to various types of pressure

† Reader

‡ Professor

pulses generated from the inhomogeneity of the atmosphere or the surrounding fluid medium. Studies concerning a moving load on a cylindrical shell have been reported by Mindlin and Bleich (1953), Mann-Nachbar (1962), Jones and Bhuta (1964), Reismann (1968), Huang (1976), etc. Realizing the frequent use of orthotropic circular cylindrical shells, e.g., in design of chemical plants and nuclear powered structures, Baker and Herrmann (1966), Jain (1974), Greenberg and Stavsky (1980) and other researchers studied the various aspects of vibration of orthotropic cylindrical shells. Mangrum and Burns (1979) analyzed the dynamic response of infinitely long orthotropic cylindrical shells subjected to an axisymmetric axially moving load. The response of a cylindrical shell subjected to a non-axially symmetric moving load was considered by Liao and Kessel (1972).

None of the above cited works concerned with the buried shell structures, because in all the referred papers shell is either filled with some acoustic medium or an acoustic medium is surrounding the shell. Chonan (1981) and Datta *et al.* (1984) have studied the dynamic response of buried shell subject to a radial moving load when shell is isotropic in nature. However, the pipes of composite materials, nowadays, are gaining more popularity in pipeline systems with one important property that strengths and stiffnesses of a composite material in different directions can be controlled at the time of fabrication of composite pipes. In last decade, some papers have appeared on dynamic response of buried orthotropic cylindrical shell under moving load (e.g., Singh *et al.* 1988, 1990 & 1991). However, in all these works the response of the shell is axisymmetric in nature. But, as the orthotropic material possesses different strength and stiffness in different directions, non-axisymmetric response of orthotropic shells assumes considerable importance.

The aim of the work reported in this paper, therefore, is to study the non-axisymmetric dynamic response of orthotropic cylindrical shells embedded in a linearly elastic, homogeneous and isotropic medium. A thick shell theory including the effects of rotary inertia and shear deformation has been used. The excitation has been taken in the form of an unsymmetric radial line load moving along the axis of the shell. The shell has perfectly been bonded to the surrounding continuum of infinite extent. Results have been obtained for very hard (rocky), medium hard and soft soil surrounding the shell. For different orthotropic parameters the flexural mode u ($n=1$) response has been compared with that of the axisymmetric mode ($n=0$). It is found that, depending upon the soil condition the shell deformation in flexural mode may be even greater than that in the axisymmetric mode. Thus, for orthotropic shells, non-axisymmetric response becomes quite important. However, the shell response is found to be significantly influenced due to variation of surrounding soil condition as well as by the orthotropy parameters.

2. Formulation of the problem

In the shell theory a co-ordinate system is employed by forming two axes in the middle surface of the shell and third axis is always normal to the middle surface. So, a cylindrical-polar co-ordinate system (r, θ, x) is defined such that x coincides with the axis of the shell and z is measured normal to the shell middle surface,

$$z = r - R, \quad -h/2 \leq r \leq h/2 \quad (1)$$

The equation governing the non-axisymmetric motion of a cylindrical shell can be written as (Mirsky and Herrmann 1957),

$$[L] \{U\} + \{P^*\} = \{0\} \quad (2)$$

where $[L]$ is a (5×5) matrix operator with terms

$$\begin{aligned} L_{11} &= k_x^2 G_{xz} h \frac{\partial^2}{\partial x^2} + \left(k_\theta^2 G_{z\theta} / R^2 \right) (h + I/R^2) \frac{\partial^2}{\partial \theta^2} - \left(\frac{E_p'}{R^2} + \frac{D'}{R^4} \right) \rho h \frac{\partial^2}{\partial t^2} \\ L_{12} &= -L_{21} = - \left[\left(k_\theta^2 \frac{G_{z\theta}}{R^2} \right) (h + I/R^2) + \left(\frac{E_p'}{R^2} + \frac{D'}{R^4} \right) \right] \frac{\partial}{\partial \theta} \\ L_{13} &= -L_{31} = \left[\frac{D'}{R^3} + \left(k_\theta^2 \frac{G_{z\theta}}{R} \right) + (h + I/R^2) \right] \frac{\partial}{\partial \theta} \\ L_{14} &= -L_{41} = - \frac{E_p v_{\theta x}}{R} \frac{\partial}{\partial x} \\ L_{15} &= L_{51} = k_x^2 G_{xz} h \frac{\partial}{\partial x} \\ L_{22} &= G_{x\theta} h \frac{\partial^2}{\partial x^2} + \left(\frac{E_p'}{R^2} + \frac{D'}{R^4} \right) \frac{\partial^2}{\partial \theta^2} - (k_\theta^2 G_{z\theta} / R^2) (h + I/R^2) - \rho h \frac{\partial^2}{\partial t^2} \\ L_{23} &= L_{32} = \frac{G_{z\theta} I}{R} \frac{\partial^2}{\partial x^2} - \frac{D'}{R^3} \frac{\partial^2}{\partial \theta^2} + (k_\theta^2 G_{z\theta} / R) (h + I/R^2) - (\rho I / R) \frac{\partial^2}{\partial t^2} \\ L_{24} &= L_{42} = \frac{1}{R} (E_p v_{\theta x} + G_{x\theta} h) \frac{\partial^2}{\partial x \partial \theta} \\ L_{25} &= L_{52} = 0 \\ L_{33} &= G_{x\theta} I \frac{\partial^2}{\partial x^2} + \frac{D'}{R^2} \frac{\partial^2}{\partial \theta^2} - (k_\theta^2 G_{z\theta}) (h + I/R^2) - \rho I \frac{\partial^2}{\partial t^2} \\ L_{34} &= L_{43} = 0 \\ L_{35} &= L_{53} = \frac{1}{R} (D v_{\theta x} + G_{x\theta} h^3 / 12) \frac{\partial^2}{\partial x \partial \theta} \\ L_{44} &= E_p \frac{\partial^2}{\partial x^2} + \frac{G_{x\theta} h}{R^2} (1 + I/hR^2) \frac{\partial^2}{\partial \theta^2} - \rho h \frac{\partial^2}{\partial t^2} \\ L_{45} &= L_{54} = \frac{D}{R} \frac{\partial^2}{\partial x^2} - \frac{G_{x\theta} I}{R^3} \frac{\partial^2}{\partial \theta^2} - (\rho I / R) \frac{\partial^2}{\partial t^2} \\ L_{55} &= D \frac{\partial^2}{\partial x^2} + \frac{G_{x\theta} I}{R^2} \frac{\partial^2}{\partial \theta^2} - k_x^2 G_{xz} h - \rho I \frac{\partial^2}{\partial t^2} \end{aligned}$$

and

$$\{U\} = [w \ v \ \psi_\theta \ u \ \psi_x]^T$$

In the above expressions w , v and u are the displacement components of the middle surface of the shell in radial, tangential and axial directions respectively, with ψ_θ and ψ_x as the angles of rotation of a straight line initially normal to the middle surface of the shell in the tangential and axial directions, respectively.

The $\{P^*\}$ are the traction components per unit area exerted on the surface of the shell and

caused due to radial moving load and also due to the scattered field created in the surrounding medium. The elements of $\{P^*\}$ are given as

$$\begin{aligned} P_1^* &= (1+z/R) \sigma_{zz} \big|_{r=R+h/2} & P_2^* &= (1+z/R) \sigma_{z\theta} \big|_{r=R+h/2}, \\ P_3^* &= z(1+z/R) \sigma_{z\theta} \big|_{r=R+h/2}, & P_4^* &= (1+z/R) \sigma_{zx} \big|_{r=R+h/2}, \\ P_5^* &= z(1+z/R) \sigma_{zx} \big|_{r=R+h/2}, \end{aligned}$$

where σ_{ij} denotes stresses with their usual meaning.

The constants appearing in the expressions for L_{ij} are defined as

$E_p = \frac{E_x h}{1 - \nu_{x\theta} \nu_{\theta x}}$, $E_p' = \frac{E_\theta h}{1 - \nu_{x\theta} \nu_{\theta x}}$, $D = E_p h^2/12$, $D' = E_p' h^2/12$, $I = h^3/12$ and $k_x = k_\theta = \pi/\sqrt{12}$ (shear correction factor), where E_x , E_θ are elastic moduli, $\nu_{x\theta}$, $\nu_{\theta x}$ the Poisson's ratios, $G_{x\theta}$, G_{xz} and $G_{z\theta}$ the shear moduli and ρ is the density of the shell material.

For evaluation of $\{P^*\}$, the stresses σ_{ij} at the outer surface of the shell (i.e., $z=h/2$) are determined in terms of scattered fields in the surrounding medium.

For any disturbance propagating in the medium, displacement $\underline{d}(r, \theta, x, t)$ at any point in the surrounding medium satisfies the equation of motion

$$c_1^2 \nabla (\nabla \cdot \underline{d}) - c_2^2 \nabla \wedge \nabla \wedge \underline{d} = \frac{\partial^2}{\partial t^2} (\underline{d}) \quad (3)$$

where, $c_1 = ((\lambda + 2\mu)/\rho_m)^{1/2}$ and $c_2 = (\mu/\rho_m)^{1/2}$ are respectively, the longitudinal and shear wave speeds depending of the values of Lamé's constants λ and μ , and density, ρ_m of the medium.

By solving this wave equation in the surrounding infinite medium, the components of the scattered fields for the n th mode ($n=0$ and $n \neq 0$ for axisymmetric and non-axisymmetric modes, respectively) can be written as

$$\begin{aligned} d_r^{(s)} &= \left[\left\{ \gamma K_n' \left(\gamma \frac{r}{R} \right) \right\} B_2 + \left\{ -i \beta \delta K_n' \left(\delta \frac{r}{R} \right) \right\} B_4 + \left\{ n (R/r) K_n \left(\delta \frac{r}{R} \right) \right\} B_6 \right] \\ &\quad \cos n \theta \exp. [i \xi (x - ct)], \\ d_\theta^{(s)} &= \left[\left\{ -n (R/r) K_n \left(\gamma \frac{r}{R} \right) \right\} B_2 + \left\{ -i n (R/r) \beta K_n \left(\delta \frac{r}{R} \right) \right\} B_4 + \left\{ -\delta K_n' \left(\delta \frac{r}{R} \right) \right\} B_6 \right] \\ &\quad \sin n \theta \exp. [i \xi (x - ct)], \\ d_x^{(s)} &= \left[\left\{ i \beta K_n \left(\gamma \frac{r}{R} \right) \right\} B_2 + \left\{ \delta^2 K_n \left(\delta \frac{r}{R} \right) \right\} B_4 \right] \cos n \theta \exp. [i \xi (x - ct)] \end{aligned} \quad (4)$$

where $d_r^{(s)}$, $d_\theta^{(s)}$ and $d_x^{(s)}$ are the components of the scattered field displacements. K_n is modified Bessel functions of the second kind, which is due to scattered wave,

$$\beta = \xi R = 2\pi R / \Lambda, \quad \gamma = (\beta^2 - \varepsilon_1^2)^{1/2}, \quad \delta = (\beta^2 - \varepsilon_2^2)^{1/2}, \quad \varepsilon_1 = \beta \frac{c}{c_1}, \quad \varepsilon_2 = \beta \frac{c}{c_2}.$$

$\Lambda (= 2\pi/\xi)$ is wavelength and $c (= \omega/\xi)$ is the speed of the moving load; B_2 , B_4 and B_6 are arbitrary constants. (') denotes differentiation with respect to the arguments of the Bessel functions.

Stress field due to scattered wave can be obtained by plugging Eq. (4) into the stress-

displacement relation of the medium, and is given by,

$$\begin{aligned}\sigma_r^{(s)} &= \frac{\mu}{R} \left[\left\{ (2\varepsilon_1^2 - \varepsilon_2^2) K_n(\gamma r/R) + 2\gamma^2 K_n''(\gamma r/R) \right\} B_2 + \left\{ -2i\beta \delta^2 K_n''(\delta r/R) \right\} B_4 \right. \\ &\quad \left. + 2n(R/r) \left\{ \delta K_n'(\delta r/R) - (R/r) K_n(\delta r/R) \right\} B_6 \right] \cos n\theta \exp.[i\xi(x-ct)] \\ \sigma_{r\theta}^{(s)} &= \frac{\mu}{R} \left[2n(R/r) \left\{ (R/r) K_n(\gamma r/R) - \gamma K_n'(\gamma r/R) \right\} B_2 + 2in(R/r)\beta \right. \\ &\quad \left\{ \delta K_n'(\delta r/R) - (R/r) K_n(\delta r/R) \right\} B_4 + \left\{ -\delta^2 K_n''(\delta r/R) + \delta(R/r) \right. \\ &\quad \left. K_n'(\delta r/R) - (nR/r)^2 K_n(\delta r/R) \right\} B_6 \left. \right] \sin n\theta \exp.[i\xi(x-ct)] \\ \sigma_{rx}^{(s)} &= \frac{\mu}{R} \left[\left\{ 2i\beta \gamma K_n'(\gamma r/R) \right\} B_2 + \left\{ \delta(2\beta^2 - \beta_2^2) K_n'(\delta r/R) \right\} B_4 \right. \\ &\quad \left. + \left\{ in(R/r)\beta K_n(\delta r/R) \right\} B_6 \right] \cos n\theta \exp.[i\xi(x-ct)]\end{aligned}$$

Stresses in the medium at the outer surface of the shell ($z=h/2$ or $r=R+h/2$) can now be obtained.

As the shell is being subjected to a radial moving load only, so for the calculations of P_1^* , the radial stress at the outer surface is written as

$$\sigma_{rr} \big|_{r=R+h/2} = \sigma_r^{(s)} \big|_{r=R+h/2} + \frac{P_{or}(\theta)}{(R+h/2)} \delta(x-ct)$$

where, $P_{or}(\theta)$ is the intensity of the applied radial line load (force per unit length) and is the function of θ . $\delta(\)$ is the Dirac delta function defined as

$$\begin{aligned}\delta(x-ct) &= 1, \text{ at } x=ct \\ &= 0, \text{ for all the values except at } x=ct\end{aligned}$$

$P_{or}(\theta)$ can be written as

$$= \sum_{n=0}^{\infty} P_n \cos n\theta$$

and then stresses generated at the outer surface of the shell are written,

$$\begin{aligned}\sigma_{rr} \big|_{r=R+h/2} &= \sigma_r^{(s)} \big|_{r=R+h/2} + \frac{P_n}{R+h/2} \cos n\theta \sigma(x-ct) \\ \sigma_{r\theta} \big|_{r=R+h/2} &= \sigma_{r\theta}^{(s)} \big|_{r=R+h/2} + 0 \quad \sigma_{rx} \big|_{r=R+h/2} = \sigma_{rx}^{(s)} \big|_{r=R+h/2} + 0\end{aligned} \quad (6)$$

and thus $\{P^*\}$ in Eq. (2) is evaluated.

Now the shell displacements are assumed to be of the forms

$$\begin{aligned}
w &= w_0 \cos n \theta \exp [i \xi(x-ct)] \\
v &= v_0 \sin n \theta [i \xi(x-ct)] \\
u &= u_0 \cos n \theta \exp [i \xi(x-ct)] \\
\psi_x &= \psi_{x0} \cos n \theta [i \xi(x-ct)]
\end{aligned}$$

and

$$\psi_\theta = \psi_{\theta 0} \sin n \theta \exp[i \xi(x-ct)] \quad (7)$$

These displacements equations along with $\{P^*\}$ are substituted into Eq. (2) to yield a set of five simultaneous equation. Three more equations are obtained by enforcing the boundary conditions at the outer surface of the shell as,

$$\begin{aligned}
w &= d_r^{(s)} \big|_{r=R+h/2} \\
v + (h/2) \psi_\theta &= d_\theta^{(s)} \big|_{r=R+h/2} \\
u + (h/2) \psi_x &= d_x^{(s)} \big|_{r=R+h/2}
\end{aligned} \quad (8)$$

Using Eqs. (2) and (7), Eq. (8) yield a set of three algebraic equations. The eight algebraic equations, thus obtained, can be presented in a matrix form to yield the final response equation which is given as

$$[Q] \{ \bar{U} \} = \{ \bar{Z} \} \delta(x-ct) \exp\{-i \xi(x-ct)\} \quad (9)$$

where $[Q]$ is a (8×8) matrix and $\{ \bar{Z} \}$ is (8×1) matrix. The elements of these matrices are as follows:

$$\begin{aligned}
Q_{11} &= -\bar{h} [k_x^2 \beta^2 + (1+\bar{h}^2/12)(n^2 k_\theta^2 \eta_4 + \eta_1 N)/\eta_2] + \Omega^2 \\
Q_{12} &= -n\bar{h} [(1+\bar{h}^2/12)(k_\theta^2 \eta_4 + \eta_1 N)]/\eta_2 \\
Q_{13} &= 2n [(\bar{h}^2/12)\eta_1 N + (1+\bar{h}^2/12)k_\theta^2 \eta_4]/\eta_2, \quad Q_{14} = -i(v_{\theta x} N/\eta_2)\bar{h} \beta \\
Q_{15} &= 2ik_x^2 \beta, \quad Q_{16} = (1+\bar{h}/2)\bar{\mu}[(2\varepsilon_1^2 - \varepsilon_2^2)K_n(\alpha_1) + 2\gamma^2 K_n''(\alpha_1)] \\
Q_{17} &= (1+\bar{h}/2)\bar{\mu}[-2i\beta\delta^2 K_n''(\alpha_2)] \\
Q_{18} &= (1+\bar{h}/2)\bar{\mu}[2n\{\alpha_2 K_n'(\alpha_2) - K_n(\alpha_2)\}/(1+\bar{h}/2)^2] \\
Q_{21} &= Q_{12}, \quad Q_{22} = -\bar{h} [\eta_3 \beta^2 + (1+\bar{h}^2/12)(k_\theta^2 \eta_4 + \eta_1 N n^2)]/\eta_2 + \Omega^2 \\
Q_{23} &= [(\bar{h}^2/6)(n^2 \eta_1 N - \eta_3 \beta^2) + (2+\bar{h}^2/6)k_\theta^2 \eta_4]/\eta_2 + (\bar{h}/6) \Omega^2 \\
Q_{24} &= -i n \bar{h} \beta (v_{\theta x} N + \eta_3)/\eta_2, \quad Q_{25} = 0 \\
Q_{26} &= (1+\bar{h}/2)\bar{\mu} [2n\{K_n(\alpha_1) - \alpha_1 K_n'(\alpha_1)\}/(1+\bar{h}/2)^2] \\
Q_{27} &= (1+\bar{h}/2)\bar{\mu} [2in\beta\{\alpha_2 K_n'(\alpha_2) - K_n(\alpha_2)\}/(1+\bar{h}/2)^2] \\
Q_{28} &= (1+\bar{h}/2)\bar{\mu} [\{\delta(1+\bar{h}/2)\}K_n'(\alpha_2) - \delta^2 K_n''(\alpha_2) - \{n^2/(1+\bar{h}/2)^2\}K_n(\alpha_2)] \\
Q_{31} &= Q_{13}, \quad Q_{32} = Q_{23} \\
Q_{33} &= -[(\bar{h}/3)(\eta_3 \beta^2 + n^2 \eta_1 N) + \{(4/\bar{h}) + (\bar{h}/3)\}k_\theta^2 \eta_4]/\eta_2 + (\Omega^2/3) \\
Q_{34} &= 0, \quad Q_{35} = -i n \bar{h} \beta (v_{\theta x} N + \eta_3)/(3\eta_2) \\
Q_{36} &= Q_{26}, \quad Q_{37} = Q_{27}, \quad Q_{38} = Q_{28} \\
Q_{41} &= -Q_{14}, \quad Q_{42} = -Q_{24}, \quad Q_{43} = Q_{34}, \quad Q_{44} = -\bar{h} \{N\beta^2 + (1+\bar{h}^2/12)n^2 \eta_3\}/\eta_2 + \Omega^2 \\
Q_{45} &= (\bar{h}/6)[\{\bar{h}(n^2 \eta_3 - N\beta^2)\}/\eta_2 + \Omega^2], \quad Q_{46} = (1+\bar{h}/2)\bar{\mu} [2i\beta\gamma K_n'(\alpha_1)] \\
Q_{47} &= (1+\bar{h}/2)\bar{\mu} [\delta(2\beta^2 - \varepsilon_2^2)K_n'(\alpha_2)]
\end{aligned}$$

$$\begin{aligned}
Q_{48} &= (1+\bar{h}/2) \bar{\mu} [in \beta K_n(\alpha_2)/(1+\bar{h}/2)] \\
Q_{51} &= -Q_{15}, \quad Q_{52} = Q_{25}, \quad Q_{53} = -Q_{35}, \quad Q_{54} = Q_{45} \\
Q_{55} &= -\{\bar{h}(N\beta^2 + n^2\eta_3)(3\eta_2)\} - (4k_x^2/\bar{h}) + (\Omega^2/3) \\
Q_{56} &= Q_{46}, \quad Q_{57} = Q_{47}, \quad Q_{58} = Q_{48} \\
Q_{61} &= 1, \quad Q_{62} = Q_{63} = Q_{64} = Q_{65} = 0, \quad Q_{66} = -\gamma K_n'(\alpha_1) \\
Q_{67} &= i\beta \delta K_n'(\alpha_2), \quad Q_{68} = -n K_n(\alpha_2)/(1+\bar{h}/2) \\
Q_{71} &= 0, \quad Q_{72} = Q_{73} = 1, \quad Q_{74} = Q_{75} = 0 \\
Q_{76} &= nK_n(\alpha_1)/(1+\bar{h}/2), \quad Q_{77} = -in\beta K_n(\alpha_2)/(1+\bar{h}/2), \quad Q_{78} = \delta K_n'(\alpha_2) \\
Q_{81} &= Q_{82} = Q_{83} = 0, \quad Q_{84} = Q_{85} = 1, \quad Q_{86} = -i\beta K_n(\alpha_1) \\
Q_{87} &= -\delta^2 K_n(\alpha_2), \quad Q_{88} = 0, \\
\{\bar{U}\} &= [\bar{W} \quad \bar{V} \quad \bar{\psi}_\theta \quad \bar{U} \quad \bar{\psi}_x \quad \bar{B}_2 \quad \bar{B}_4 \quad \bar{B}_6]^T \text{ in which} \\
\bar{W} &= \frac{w_o G_{xz}}{P_n}, \quad \bar{V} = \frac{v_o G_{xz}}{P_n}, \quad \bar{\psi}_\theta = \frac{h \psi_{\theta o} G_{xz}}{2P_n}, \quad \bar{U} = \frac{u_o G_{xz}}{P_n} \\
\bar{\psi}_x &= \frac{h \psi_{xo} G_{xz}}{2P_n}, \quad \bar{B}_2 = \frac{B_2 G_{xz}}{P_n}, \quad \bar{B}_4 = \frac{B_4 G_{xz}}{P_n}, \quad \bar{B}_6 = \frac{B_6 G_{xz}}{P_n} \\
\{\bar{Z}\} &= [-1 \ 0 \ 0 \ 0 \ 0 \ 0 \ 0 \ 0]^T
\end{aligned}$$

where $\bar{h} = h/R$, $\eta_1 = \frac{E_\theta}{E_x}$, $\eta_2 = \frac{G_{xz}}{E_x}$, $\eta_3 = \frac{G_{x\theta}}{E_x}$, $\eta_4 = \frac{G_{z\theta}}{E_x}$

$$\begin{aligned}
N &= 1/(1 - v_{x\theta} v_{\theta x}), \quad \bar{\mu} = \mu G_{xz}, \quad \Omega^2 = \rho h \omega^2 \frac{R}{G_{xz}} = \bar{h} \bar{\mu} \varepsilon_z^2 \bar{\rho} \\
\bar{\rho} &= \rho_m/\rho, \quad \alpha_1 = (1+\bar{h}/2)\gamma, \quad \alpha_2 = (1+\bar{h}/2)\delta
\end{aligned}$$

Now a new moving coordinate is defined as

$$\bar{X} = \frac{(x-ct)}{R} \quad (10)$$

and the Fourier transform given by

$$f^*(\beta) = \int_{-\infty}^{\infty} f(\bar{X}) e^{i\beta\bar{X}} d\bar{X} \quad (11)$$

and

$$f(\bar{X}) = \frac{1}{2\pi} \int_{-\infty}^{\infty} f^*(\beta) e^{-i\beta\bar{X}} d\beta \quad (12)$$

is used in Eq. (9). With this transformation the matrix Eq. (9) become

$$[Q] \{\bar{U}^*\} = \{\bar{Z}\} \quad (13)$$

Now the matrix Eq. (13) can be solved to get the value \bar{W}^* of column matrix $\{\bar{U}^*\}$. To get back the value \bar{W} i.e., the radial displacement from \bar{W}^* , inverse transformation given in Eq. (12) is used.

3. Results and discussions

The results are presented for a transversely isotropic shell with $r - \theta$ as the plane of isotropy.

Accordingly, $E_\theta = E_z$, $G_{xz} = G_{x\theta}$, $v_{\theta z} = v_{z\theta}$, $v_{x\theta} = v_{xz}$ and $G_{z\theta} = E_\theta/2(1+v_{\theta z})$. Thus, we have $\eta_2 = \eta_3$ and $\eta_4 = G_{z\theta}/E_x = \eta_1/2(1+v_{\theta z})$. $v_{\theta z}$ and $v_{x\theta}$ have been taken as 0.3 for numerical calculations. These different values of η_1 and η_3 used in the results are as follows:

$$\eta_1 = 0.05, 0.10 \text{ and } 0.50$$

$$\eta_3 = 0.02, 0.05 \text{ and } 0.10$$

These values are expected to cover a wide range of orthotropic materials. While studying the effect of one orthotropy parameter the other one is kept constant.

To simulate all kinds of combinations of ground and pipe, the rigidity ratio $\bar{\mu}$ has been varied between 0.10 and 10. $\bar{\mu}=0.10$ corresponds to soft soil whereas $\bar{\mu}=10$ represents hard and rocky surrounding medium. For all the value of $\bar{\mu}$, the Poisson's ratio of the medium, v_m , has been assumed as 0.25. Thickness to radius ratio of the shell (\bar{h}) has been taken as 0.05 and density ratio of the surrounding medium to that of the shell ($\bar{\rho}$) has been taken as 0.30. Non-dimensional amplitudes of the middle surface of the shell in the radial and axial directions (\bar{W} and \bar{U}) have been plotted against \bar{x} at a load speed, $\bar{C}=0.10$.

Figs. 1 and 2, respectively, show the variation of radial deformation (\bar{W}) with (\bar{x}) for soft surrounding soil ($\bar{\mu}=0.10$) and with η_1 and η_3 as parameters. Figures show that radial deformation is maximum under the load (i.e., (\bar{x})=0) and decreases as (\bar{x}) approaches 0.5. It is observed that when shell is surrounded by very soft soil the flexural mode response is predominant over the axisymmetric response. It can also be seen that the variations in η_1 and η_3 have strong influence on radial displacement and this influence is relatively more in axisymmetric mode. Figures show that with increase in η_1 , \bar{W} decreases, whereas it increases with increase in η_3 , and this behaviour is similar in both the modes. Ahead of the load the difference in displacement pattern due to variation of η_1 or η_3 goes on shrinking and it is very narrow in flexural mode when (\bar{x})

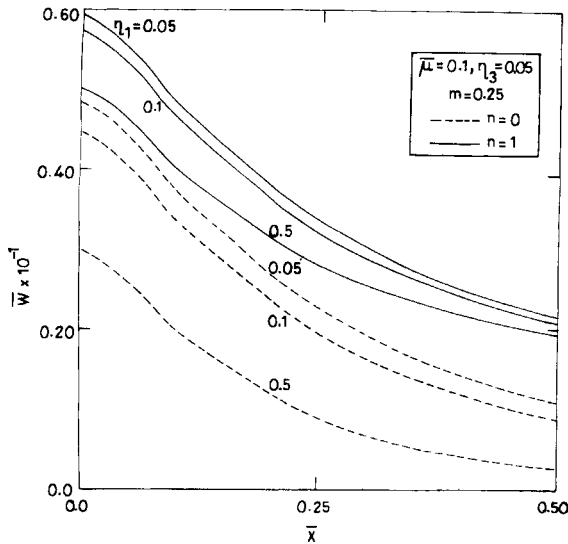


Fig. 1 Radial displacement (\bar{W}) versus non-dimensional moving axial coordinate (\bar{x}) at $\bar{C}=0.10$ with η_1 as parameter at $\bar{\mu}=0.10$

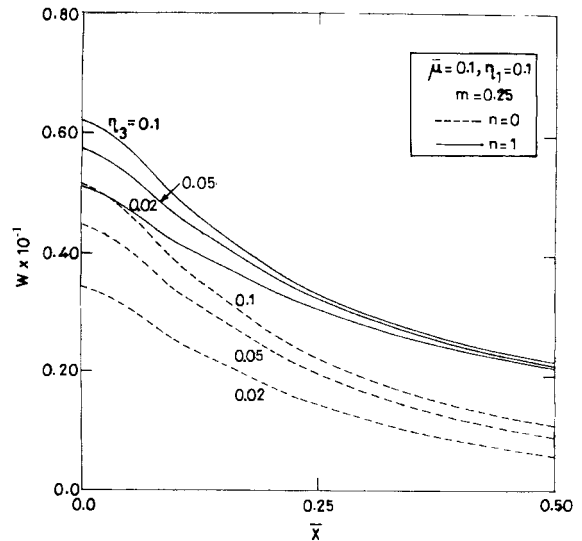


Fig. 2 Radial displacement (\bar{W}) versus non-dimensional moving axial coordinate (\bar{x}) at $\bar{C}=0.10$ with η_3 as parameter at $\bar{\mu}=0.10$

approaches 0.5.

Figs. 3 and 4 have been plotted when rigidity moduli of surrounding soil and the shell are comparable (i.e., $\bar{\mu} = 1.0$). Here also it is observed that flexural mode response dominates the axisymmetric mode response. But, compare to the soft surrounding soil condition, the differences in \bar{W} between two modes, here, is very small. It is evident from the figures that η_1 or η_3 has very small influence on \bar{W} in both the modes. However, the difference in \bar{W} due to change of mode is more remarkable than the variation of orthotropy parameters. The maximum radial displacement under the load is not much affected due to variation of orthotropy parameters. Figs. 5 and 6 are drawn to show the behaviour of radial displacement with η_1 and η_3 , respectively, as parameters. Figures show that when shell is buried in very hard or rocky surrounding soil ($\bar{\mu} = 10$), the radial displacement \bar{W} , is not affected due to changes in η_1 or η_3 . However, the flexural mode response is predominant over axisymmetric mode response. This difference is small but increases slowly as \bar{x} approaches 0.5. So, in hard and rocky surrounding soil the introduction of orthotropy through the parameters η_1 and η_3 does not bring any difference in \bar{W} , whereas, \bar{W} is affected as response mode is changed.

Figs. 7-12 have been drawn for axial displacement (\bar{U}) of the shell in the axisymmetric ($n=0$) and the flexural mode ($n=1$) with η_1 , η_3 and $\bar{\mu}$ as parameters.

Figs. 7 and 8 show, with η_1 and η_3 , respectively as parameters the variation of the axial deformation of the middle surface of the shell (\bar{U}) with (\bar{x}), when soil surrounding the shell is very soft ($\bar{\mu} = 0.10$). It is seen from figures that the amplitude of the axial deformation in axisymmetric mode is very high as compared to the flexural mode response. The rate of decay of displacement amplitude is similar for both the orthotropic parameters and in both the response modes. The difference in \bar{U} , due to changes in η_1 or η_3 appears to be shrinking as (\bar{x}) approaches

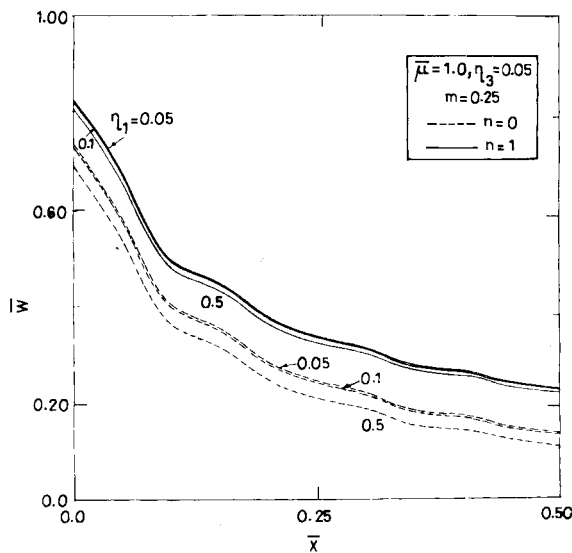


Fig. 3 Radial displacement (\bar{W}) versus non-dimensional moving axial coordinate (\bar{x}) at $\bar{C} = 0.10$ with η_1 as parameter at $\bar{\mu} = 1.0$

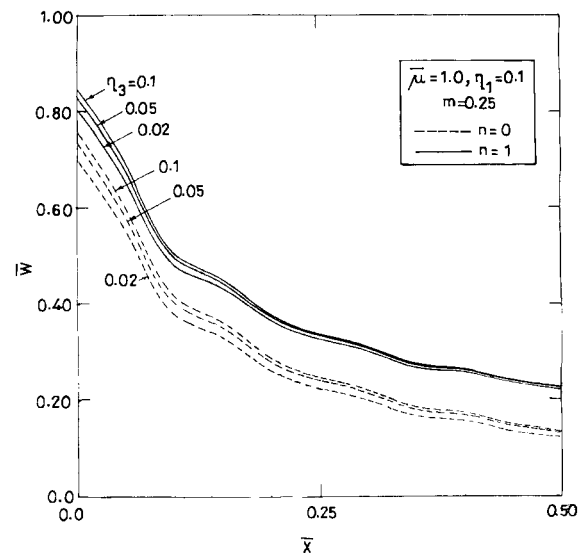


Fig. 4 Radial displacement (\bar{W}) versus non-dimensional moving axial coordinate (\bar{x}) at $\bar{C} = 0.10$ with η_3 as parameter at $\bar{\mu} = 1.0$

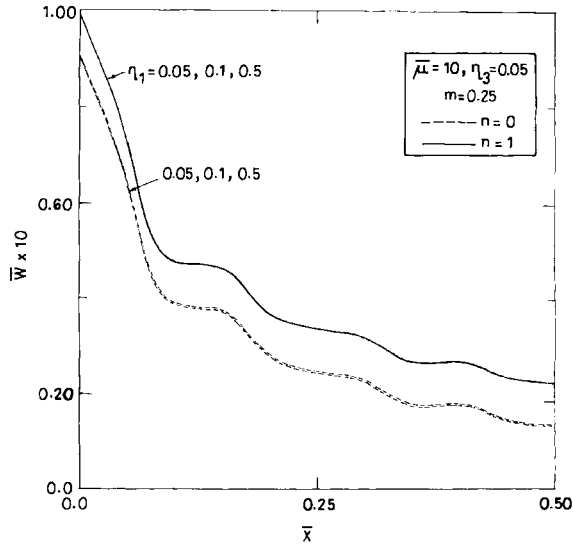


Fig. 5 Radial displacement (\bar{W}) versus non-dimensional moving axial coordinate (\bar{x}) at $\bar{C}=0.10$ with η_1 as parameter at $\bar{\mu}=10$

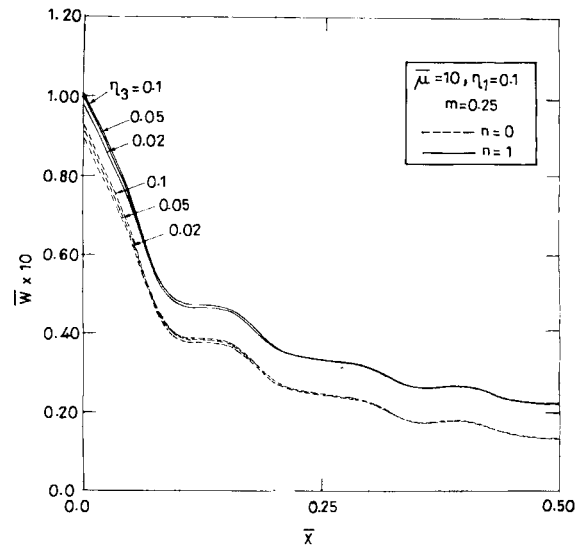


Fig. 6 Radial displacement (\bar{W}) versus non-dimensional moving axial coordinate (\bar{x}) at $\bar{C}=0.10$ with η_3 as parameter at $\bar{\mu}=10$

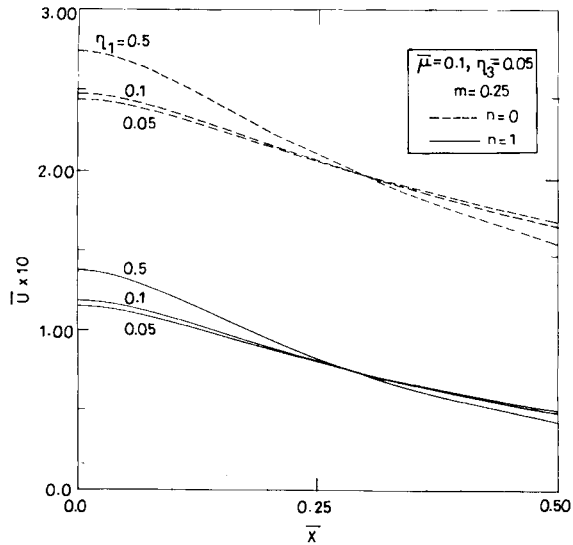


Fig. 7 Axial displacement (\bar{U}) versus non-dimensional moving axial coordinate (\bar{x}) at $\bar{C}=0.10$ with η_1 as parameter at $\bar{\mu}=0.10$

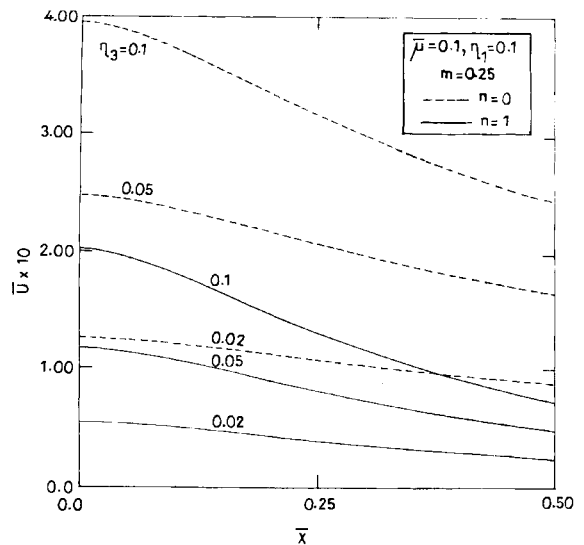


Fig. 8 Axial displacement (\bar{U}) versus non-dimensional moving axial coordinate (\bar{x}) at $\bar{C}=0.10$ with η_3 as parameter at $\bar{\mu}=0.10$

0.5. From figures it is evident that orthotropy parameter η_1 has small influence on \bar{U} as compared to η_3 in both axisymmetric as well as flexural modes. It can be seen that the maximum axial displacement under the load can be reduced to an appreciable level by decreasing the value of η_3 . Therefore, in soft surrounding soil the axial deformation under the load can be reduced to a remarkably low level by choosing a proper combination of orthotropic parameters. The

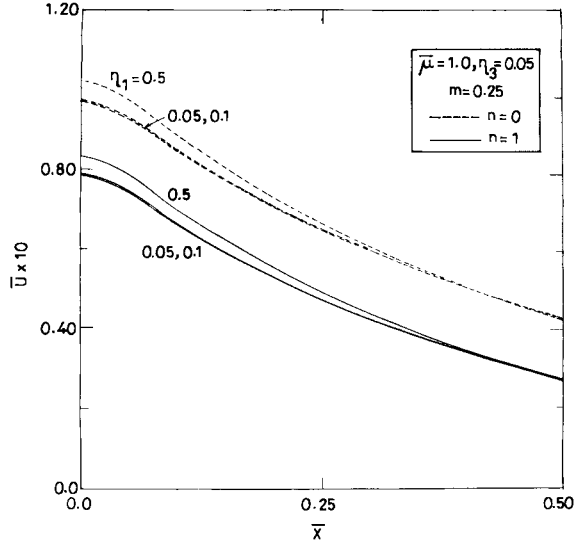


Fig. 9 Axial displacement (\bar{U}) versus non-dimensional moving axial coordinate (\bar{x}) at $\bar{C}=0.10$ with η_1 as parameter at $\bar{\mu}=1.0$

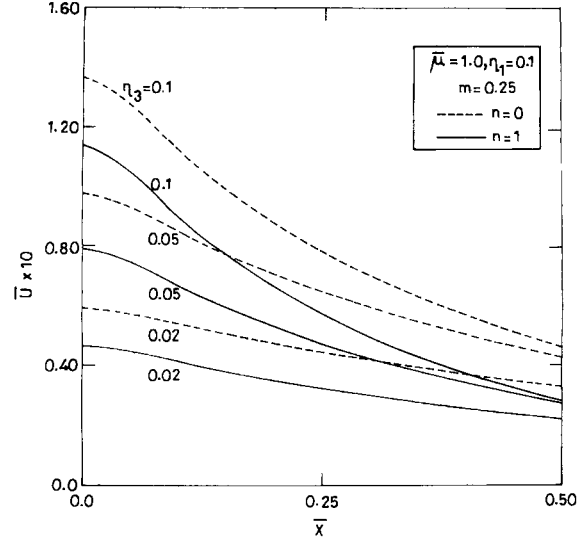


Fig. 10 Axial displacement (\bar{U}) versus non-dimensional moving axial coordinate (\bar{x}) at $\bar{C}=0.10$ with η_3 as parameter at $\bar{\mu}=1.0$

observation is true for axisymmetric as well as flexural mode response.

Figs. 9-12 indicate that when shell is buried under medium hard ($\bar{\mu}=1.0$) or very hard and rocky ($\bar{\mu}=10$) surrounding medium the axial deformation \bar{U} , is maximum in axisymmetric mode than in flexural mode. This behaviour of the response is true with both the orthotropy parameters,

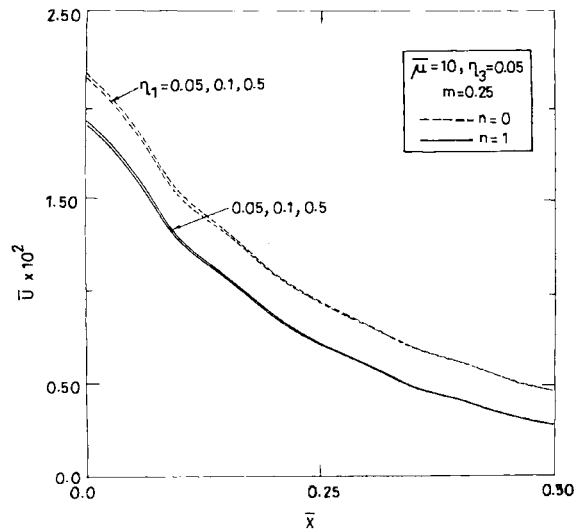


Fig. 11 Axial displacement (\bar{U}) versus non-dimensional moving axial coordinate (\bar{x}) at $\bar{C}=0.10$ with η_1 as parameter at $\bar{\mu}=10.0$

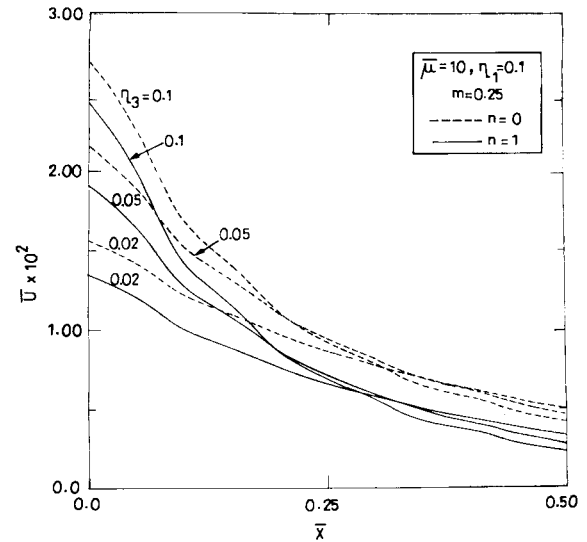


Fig. 12 Axial displacement (\bar{U}) versus non-dimensional moving axial coordinate (\bar{x}) at $\bar{C}=0.10$ with η_3 as parameter at $\bar{\mu}=10.0$

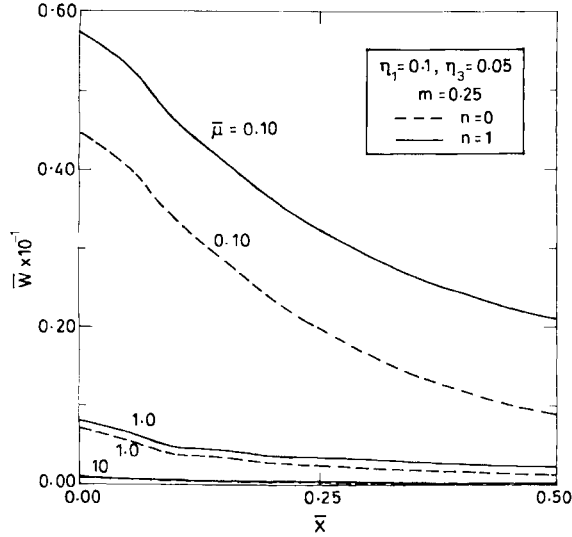


Fig. 13 Radial displacement (\bar{W}) versus non-dimensional moving axial coordinate (\bar{x}) at $\bar{C}=0.10$ with $\bar{\mu}$ as parameter

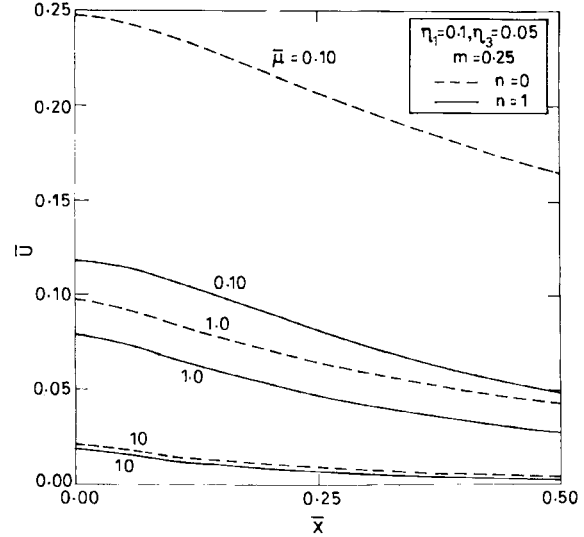


Fig. 14 Axial displacement (\bar{U}) versus non-dimensional moving axial coordinate (\bar{x}) at $\bar{C}=0.10$ with $\bar{\mu}$ as parameter

η_1 and η_3 . The maximum response under the load goes on reducing as \bar{X} approaches 0.5. In both the response modes variation in η_1 does not bring any appreciable change in axial displacement, whereas changes in η_3 make remarkable difference in \bar{U} and this difference narrows down as \bar{X} increases. Increase in η_3 increases \bar{U} . The nature of variation in \bar{U} due to changes in orthotropy parameters are similar for axisymmetric and flexural mode response. It is interpreted for both surrounding soil conditions (i.e., $\bar{\mu}=1.0$ and 10.0), that whether it is axisymmetric mode or flexural mode response the axial deformation under the load can be reduced to a remarkable level by a proper combination of orthotropy parameters η_1 and η_3 .

Figs. 13 and 14 show, respectively, the variation of \bar{W} and \bar{U} against \bar{X} for different values of $\bar{\mu}$ in both axisymmetric and flexural modes. From figures it is clear that the radial deformation \bar{W} , is always higher in flexural mode whereas axial deformation \bar{U} , is predominant in axisymmetric mode. The difference in the value of deformations (\bar{W} or \bar{U}) for the two response modes is very distinct when soil surrounding the shell is very soft and, as it appears, this difference is very significant for the axial deformation of the shell. The deformation amplitudes (\bar{W} or \bar{U}) is almost the same in both the modes.

4. Conclusions

The main finding of the work carried out in this paper may be concluded as:

- (1) Radial displacement \bar{W} due to the flexural mode response is greater than the axisymmetric mode response and this difference in \bar{W} is more significant when surrounding soil is soft.
- (2) The effect of variation of orthotropy parameters on \bar{W} is almost similar in both the modes, however, the values of \bar{W} is more sensitive to the choice of the mode than the variation in η_1 or η_3 , when surrounding soil is hard.

- (3) The axial displacement \bar{U} is large under axisymmetric mode in comparison of the flexural mode and under the load \bar{U} is significantly affected due to variation of η_3 . This behaviour is true for all the values of $\bar{\mu}$.
- (4) In general, the difference in displacements (\bar{W} or \bar{U}) due to variation of η_1 and η_3 is large when surrounding soil is soft, whereas, in hard and rocky medium the displacements have almost the same amplitudes in both the modes.
- (5) The maximum deflection under the load can be reduced by adjusting the orthotropy parameters in both the modes.

The observation that axial displacement under the load can be significantly be reduced, by changing the values, of η_3 , is of special interest because most of the failure of buried pipes have been reported as due to excessive axial displacements.

References

- Baker, E.H. and Herrmann, G. (1966), "Vibration of orthotropic cylindrical sandwich shells under initial stress", *AIAA*, **4**, 1063-1070.
- Chonan, S. (1981), "Dynamic response of a cylindrical shell imperfectly bonded to a surrounding continuum of infinite extent", *J. Sound Vib.*, **78**, 257-267.
- Datta, S.K. and Chakraborty, T. (1984), "Dynamic response of pipelines to moving loads", *Int. J. Earthqk. Engg. Struct. Dyn.*, **12**, 59-72.
- Greenberg, J.B. and Stavsky, Y. (1980), "Buckling and vibration of orthotropic composite cylindrical shells", *Acta Mechanica*, **36**, 15-29.
- Huang, C.C. (1976), "Moving loads on elastic cylindrical shells", *J. Sound Vib.*, **49**, 215-220.
- Jain, R.A. (1974), "Vibration of fluid-filled, orthotropic cylindrical shells", *J. Sound Vib.*, **37**, 379-388.
- Jones, J.P. and Bhuta, P.G. (1964), "Response of cylindrical shells to moving loads", *ASME J. Appl. Mech.*, **31**, 105-111.
- Kota, V.N. and Singh, V.P. (1991), "Effect of presence of fluid on the dynamic response of buried orthotropic cylindrical shells under a moving load", *J. Thin-Walled Struct.*, **12**, 256-279.
- Liao, E.N.K. and Kessel, P.G. (1972), "Response of pressurized cylindrical shells subjected to moving loads", *ASME J. Appl. Mech.*, **39**, 227-234.
- Mangrum, E. and Burns, J.J. (1979), "Orthotropic cylindrical shells under dynamic loading", *ASME J. Mech. Des.*, **101**, 322-329.
- Mann-Nachbar, P. (1962), "On the role of bending in the dynamic response of thin shells to moving discontinuous loads", *J. Aerospace Sci.*, **29**, 648-657.
- Mindlin, R.D. and Bleich, H.H. (1953), "Response of an elastic cylindrical shell to a transverse, step shock wave", *ASME J. Appl. Mech.*, **20**, 189-195.
- Mirsky, I. and Herrmann, G. (1957), "Non-axially symmetric motions of cylindrical shells", *J. Acous. Soc. Am.*, **29**, 1116-1123.
- Reismann, H. (1968), "Response of a cylindrical shell to an inclined, moving pressure discontinuity", *J. Sound Vib.*, **8**, 240-255.
- Singh, V.P., Upadhyay, P.C. and Kishore, B. (1987), "On the dynamic response of buried orthotropic cylindrical shells", *J. Sound Vib.*, **113**, 101-115.
- Singh, V.P., Upadhyay, P.C. and Kishore, B. (1988), "On the dynamic response of buried orthotropic cylindrical shells under moving load", *Int. J. Mech. Sci.*, **30**, 397-406.
- Singh, J. and Singh, V.P. (1990), "Dynamic response of buried orthotropic cylindrical shells to an inclined axisymmetric moving load", *J. Comp. Struct.*, **37**, 71-80.